Recycling 3D Printed Residues for the Development of Disposable Paper-Based Electrochemical Sensors

Habdias Silva-Neto, Gerson Duarte-Junior, Danielly Rocha, Fethi Bedioui, Anne Varenne, Wendell Coltro

Recycling 3D printed residues for the development of disposable paper-based electrochemical sensors

Habdias A. Silva-Neto[a], *Gerson F. Duarte-Junior*[a], *Danielly S. Rocha*[a] *Fethi Bedioui*[b], *Anne Varenne*[b] *and Wendell K. T. Coltro*[a,c]*

[a]Instituto de Química, Universidade Federal de Goiás, 74690-900, Goiânia, GO, Brazil

[b]Institute of Chemistry for Life and Health Sciences i-CLeHS, Chimie ParisTech-PSL/CNRS 8060, Paris, France

[c]Instituto Nacional de Ciência e Tecnologia de Bioanalítica, 13084-971, Campinas, SP, Brazil

***Corresponding Author:**

Professor Wendell K. T. Coltro

Instituto de Química, Universidade Federal de Goiás

Campus Samambaia, 74690-900

Goiânia, GO, Brazil

Fax: +55 62 3521 1127

E-mail: wendell@ufg.br

ORCID: http://orcid.org/0000-0002-4009-2291

Abstract

Here, we propose a recyclable approach using acrylonitrile-butadiene-styrene (ABS) residues from additive manufacture in combination with low-cost and accessible graphite flakes as a novel and potential mixture for creating conductive paste. The graphite particles were successfully incorporated in the recycled thermoplastic composite when solubilized with acetone and the mixture demonstrated greater adherence to different microchip substrates, among which cellulose-based substrate making possible the construction of paper-based electrochemical sensor (PES). The morphological, structural and electrochemical characterization of the recycled electrode material were demonstrated similar to the ones of the traditional carbon-based surfaces. Faradaic responses based on redox probe activity ($[Fe(CN)_6]^{3-/4-}$) exhibited well-definite peak currents, diffusional mass-transfer, as a quasi-reversible system (96 ± 5 mV) with a fast heterogeneous rate constant value of 2 x 10^{-3} cm s^{-1}. To improve the electrode electrochemical properties, both the PES and the classical 3D-printed electrode surfaces were modified with a combination of multi-walled carbon nanotubes (MWCNT), graphene oxide (GO) and copper. Both electrode surfaces demonstrated the suitable oxidation of nitrite at 0.6 and 0.5 V vs Ag, respectively. The calculated analytical sensitivity for PES and 3D-printed electrodes were 0.005 and 0.002 µA/[µmol L^{-1}], respectively. The proposed PES was applied for the indirect amperometric analysis of S-nitroso-cysteine (CysNO) in serum samples via nitrite quantitation, demonstrating a limit of detection of 4.1 µmol L^{-1}., with statistically similar values when compared to quantitative analysis of the same samples by spectrophotometry (paired t-test, 95% confidence limit). The evaluated electroanalytical approach exhibited linear nitrite concentrate range between 10 and 125 µmol L^{-1}, that is suitable for realizing clinical diagnosis involving Parkinson's disease, for example. This proof of concept shows the great promise of this recyclable strategy combining ABS residues and conductive particles in the context of green chemical protocols for constructing disposable sensors.

Keywords: Complex thermoplastic waste, 3D printing, stencil printing, green chemical principles, carbon-based electrodes, S-nitroso-cysteine.

1. Introduction

Additive manufacturing approach also nominated as 3D printing has been providing an infinite of notorious contributions, including to the civil construction, medicine and dental industry, aerospace market, automobile technology, consumer goods and electrochemical sensors.[1–4] Recently, many strategies have been proposed in the domain of printable industry for constructing individual protective equipment that can be devoted to COVID-19 for example (a reference from you?) leading to an increase in the 3D printing market. As a result and according to GlobeNewswire,[5] the materials demand involving thermoplastic filaments was proximally USD 968 million in 2021, indicating that the 3D printing technology is extremely versatile and accessible in outbreak cases.

The most usual 3D printers are based on fused depositing modeling (FDM) combined with thermoplastic filaments such as polylactic acid (PLA), polyethylene terephthalate (PET), acrylonitrile-butadiene-styrene (ABS) for successfully constructing many groundbreaking plastic objects for multiple finalities from medicine assay to chemical analysis.[6–9] Notably, these moldable devices have piqued the interest of laboratories due to some peculiarities, including low-cost, accessibility, versatility, chemical stability, mechanical resistance, hydrophobicity and most important superior quality and long utility span.[10–12] Among the previously cited filaments, PLA allows the construction of well-defined objects and is bio-degradable, however it exhibits low mechanical and thermal resistance.[13,14] On the other hand, PET and ABS are more efficient in terms of mechanical, chemical, and thermal resistance. Furthermore, ABS is considered as toxic with a low degradability.[13,15] For this reason, it is important to propose strategies to recycle those

materials following the green chemical principles to reduce or eliminate the use or generation of hazardous compounds.[16]

Highlights papers in the literature revealed that the thermoplastic materials can be reusable by numerous ways, (i) recycling carbon fibers and using them as additive option in the fused filament fabrication (FFF) process of PLA,[17] and (ii) reusing glass fiber obtained from turbine blades to reinforce the mechanical properties of PLA material.[18]. However, to the best of our knowledge, the aforementioned studies do not explore the residues of thermoplastic as binder structures for manufacturing disposable electrochemical sensors, which are of high potential in the modern analytical chemistry field, including forensic,[19,20] pharmaceutical,[12] environmental,[21,22] food and biological ones[23–25] .

In this study we propose for the first time a recyclable approach using residues of ABS as binder to prepare carbon-based conductive ink and create disposable paper-based electrochemical sensor (PES). First the proof of concept of integration of the recycled ABS mixed with graphite particle as a material for electrodes on different microchip materials was demonstrated, highlighting the efficient electrode integration on paper-based materials thanks to morphological, structural and electrochemical characterizations. To improve the faradaic response of the sensor, we developed two simple strategies: (i) removing the insulating ABS structures based on fast electrochemical oxidation; (ii) improving the catalytic electrode performance for nitrogene-based groups through modification of the electrode surface with a mixture of multi-walled carbon nanotubes, graphene oxide and copper, as well-known reported in the literature for the oxidation of nitrite.[26]

As a matter of comparison, fully 3D-printed carbon-black electrodes were also fabricated and tested in the same experimental conditions. As a further proof of concept, this disposable PES was applied for the indirect detection by chronoamperometry of S-nitroso-cysteine (CysNO) in human serum samples. This biomolecule from the S-nitrosothiols (RSNOs) group can play an essential role in several physiological and physiopathological processes, actuating as biomarker and

NO-donors.[27] This new recyclable strategy combining ABS residues and conductive particles was finally compared to to classical spectrophotometry analysis of these human serum samples.

2. Experimental

2.1 Materials and reagents

Potassium ferrocyanide, potassium ferricyanide, potassium chloride, acetic acid, acetonitrile, copper sulfate pentahydrate, sulfuric acid, sulfanilamide, N-(1-naphthyl)ethylenediamine (NED), multi-walled carbon nanotubes (MWCNT) (OD: 6–9 nm, length: 5 μm), graphene oxide (GO), sodium sulfate, iron sulfate hexahydrate, uric acid, hydrochloric acid, and cysteine were purchased from Sigma-Aldrich (Saint Louis, MO, USA). Acetone, sodium nitrite, sodium nitrate and hydrogen peroxide were acquired from Neon (Suzano, SP, Brazil). All reagents were analytical grade and used as received. The stock and standard solutions were prepared in ultrapure water processed through a purification system (Direct-Q 3, Millipore, Darmstadt, Germany) with a resistivity equal to 18.2 MΩ cm.

Vegetal paper also nonmined as waterproof (weight = 180 g m^{-2}), thermosensitive polyester films (thickness = 250 μm) and nail polish were obtained from Ecrisam (Goiânia, GO, Brazil), Yidu Group Co., (Hsi- Chih, TPE, Taiwan) and RISQUÈ® (São Paulo, SP, Brazil), respectively. Graphite powder (ø ≤ 50 μm), silver ink model PC-9070/1 and adhesive vinyl film were provided by Synth (Diadema, SP, Brazil), Joint Metal (São Paulo, SP, Brazil) and Imprimax (São Paulo, SP, Brazil), respectively. Thermoplastic filaments (ø = 1.75 mm) as acrylonitrile butadiene styrene (ABS) and polylactic acid/carbon black (PLA-CB) composite filament (brand name ProtoPasta) were supplied by 3D Fila (Belo Horizonte, MG, Brazil). Whatman® grade 1 chromatography paper (thickness: 0.18 mm) was received from Sigma-Aldrich.

2.2 Instruments

The stencil masks were designed and constructed using a cutting printer Cameo (Silhouette, Belo Horizonte, MG, Brazil) and managed by Silhouette Studio® software (version 4.1). The thermal laminator model 101118415 was acquired from Gazela (Divinópois, MG, Brasil). The layout of 3D printed electrode was designed in SolidWorks software and manufactured using an Original Prusa i3 mk2/S 3D printer (Prusa Research, Prague, Czech Republic). A portable cabin integrated with UV LED (7 W) purchased from Kiss NY Pro (New York, USA) was used to degrade CysNO samples. The electrochemical measurements were performed through a portable bipotentiostat/galvanostat, model μStat 400 (DropSens S.L., Oviedo, Spain) and monitored by DropView® software.

2.3 Collection of ABS residues, preparation of conductive ink and electrochemical sensor

ABS residues were collected from two sources: (i) during the outbreak of COVID-19 when our group successfully fabricated face shield and magnetic holder to donations in local hospitals; (ii) from microfabrication researcher involving microfluidic devices. ABS leftovers were crushed using an industrial processor (Mondial, São Paulo, Brazil) and stored in plastic bottles (see in Figure S1 available in electronic supporting information).

Next, the preparation of conductive ink based on combination of graphite flakes and ABS residues, and the fabrication of electrodes via stencil printing technique were performed in five steps. (i) The geometry of the device (auxiliary, AE; reference, RE; and working, WE, Ø = 4 mm) was designed using CorelDraw software. (ii) The stencil masks were constructed by combining the optimized substrate with polyester film (heat press at 120 °C for 5 s) followed by two layers of self-adhesive vinyl upon optimized substrate (vegetal paper). The plastic mask was performed by a reductive printing process via a cutting plotter. (iii) For realizing the synthesis of conductive ink, a mixture of 1.5 g oABS residue and 15 mL acetone were prepared and exposed to a continuous stirring process (700 rpm) for 30 min. 1.5 g graphite powder was then added to mixture and left again under stirring (700 rpm; 15 min). (iv) The conductive ink was dispersed over the stencil

mold/substrate using a spatula and after drying overnight (25 ± 2 ºC) the vinyl masks were removed. (v) Additionally, steps involving the construction of a pseudo RE, a hydrophobic barrier, and an electrochemical cleaning process were realized through painting of RE with silver ink, delimitating the target geometric area using nail polish, adding 50 µL acetic acid (6 mol L^{-1}) on the electrode surface and applying a potential of 1.8 V vs Ag for 100 s.

For realizing the comparative experiments, fully 3D-printed electrodes were manufactured, and the surface activated according to a recent study.[22]

2.4 Preparation of modified sensor surface

The WE surface modification by MWCNT/GO was realized based on three steps, as reported in a recent study.[26] (i) The MWCNT/GO composite was synthesized by dispersing 1.0 mg GO into 5.0 mL water and sonicating for one hour. After, 1.0 mg MWCNT was added and sonicated for one hour [11]. An aliquot of 10 µL of the MWCNT/GO dispersion was dropped on the electrode surface and dried by overnight (25 ± 2 ºC). (ii) The electrode was electrochemically reduced under a potential of -1.2 V vs Ag for 140 s in the presence of 0.1 mol L^{-1} H_2SO_4, as supporting electrolyte. (iii) A solution composed of 10 mmol L^{-1} Cu(II) prepared in 0.1 mol L^{-1} H_2SO_4 was dropped on the MWCNT/GO surface and a potential of -0.7 V vs Ag was applied for 200 s, for the reduction of Cu(II) ion to Cu(0).

2.5 Synthesis and decomposition procedures of S-nitrosocysteine

The synthesis of CysNO was performed as described elsewhere by Peterson.[32] Briefly, an equimolar amount of cysteine and sodium nitrite (5 mmol L^{-1}) were mixed in a dark flask (to prevent decomposition by the action of light), followed by the addition of 0.1 mol L^{-1} hydrochloric acid. After 5 minutes, 0.1 mol L^{-1} phosphate buffer (pH 7.4) prepared in 0.5 mmol L^{-1} EDTA was

added to the target solution in order to neutralize and avoid decomposition through traces of contaminating metals. The concentration of CysNO was estimated by colorimetric characterization using an UV-Vis spectrophotometer model UV-M51 from BEL Photonics (Milan, Italy). Absorption measurement was realized in a spectral scan ranging from 250 to 500 nm, highlighting a peak at a 335 nm wavelength with a ε = 719 L mol^{-1} cm^{-1} (Figure S2; available in the electronic supplementary information, SI). For the decomposition of CysNO, the solution was exposed for 15 minutes to UV-LEDs.

2.6 Electrochemical experiments

The proposed PESs were submitted to both cyclic voltammetry (CV) and amperometry analysis. CV experiments were performed in the presence of 1.0 mmol L^{-1} $[Fe(CN)_6]^{3-/4-}$ prepared in 0.1 mol L^{-1} KCl, to optimize the substrate, characterize the electrochemical response and verify the repeatability and reproducibility of the raw recycled electrodes. The catalytic performance of modified electrodes in terms of redox activity, repeatability, and reproducibility was studied using the oxidation of nitrite (1.0 mmol L^{-1} nitrite prepared in 0.1 mol L^{-1} Na_2SO_4), as a model reaction. Finally, the amperometric approach was selected for quantitation of nitrite at 0.6 V vs Ag for 50 s. As comparative experiments, electrochemical analysis was realized using 3D printed electrodes with detection conditions at 0.5 V vs Ag for 30 s. The selectivity study was also realized with a standard solution of 50 µmol L^{-1} nitrite dopped with different interfering agents (nitrate, uric acid, chloride, and Fe(II) prepared at 5 µmol L^{-1} each).

To prove the concept of the electroanalytical PES method, the electrodes were explored for analysis of CysNO in serum samples. Artificial serum was purchased from Doles (Goiânia, GO, Brazil) and the sample preparation and decomposition steps were adapted from Ismail et al.[33] Posteriorly, artificial serum samples were diluted in 0.1 mol L^{-1} Na_2SO_4 (proportion 1:5; v/v) and the samples were doped with the CysNO degraded molecule at three different concentrations, i.e. 20, 40 and 80 µmol L^{-1}. Figure 1 shows a scheme of the sensor construction process and the indirect

electrochemical detection of CysNO. All electrochemical measurements were realized at room temperature (25 ± 2 ºC).

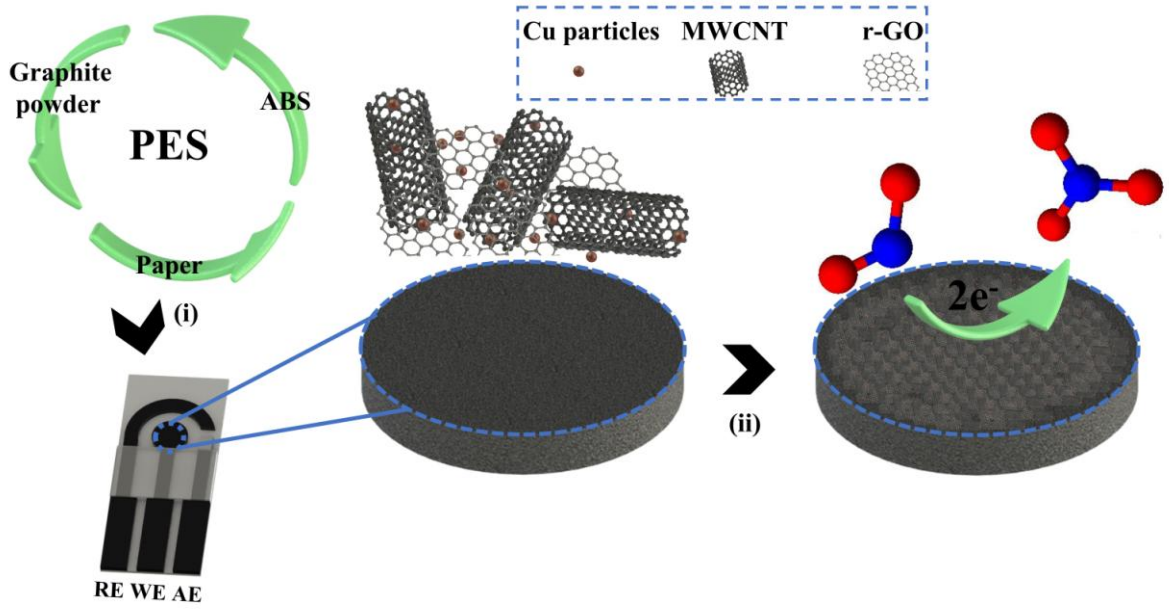

Figure 1. Schematic representation of fabrication (i) and modification of electrode aiming for sensing of nitrite (ii).

2.7 Characterization

Electrical resistance (ER), scanning electron microscopy (SEM), Raman spectroscopy and electrochemical characterization were realized. ER of conductive trail was estimated by a digital multimeter model MD-360 (INSTRUTHERM, São Paulo, Brazil). SEM analysis was performed using a JEOL microscope model JSM 6610 (Waltham, MA, USA). Raman spectroscopy was performed with a confocal Raman spectrometer model LabRAM HR Evolution (Horiba, Kyoto, Japan). Electrochemical characterization was performed from CV measurements in the presence of 1.0 mmol L^{-1} $[Fe(CN)_6]^{3-/4-}$ prepared in 0.1 mol L^{-1} KCl with a scan rate ranging from 10 to 100 mV s^{-1} at -0.6 to 0.5 V *vs* C. The procedure of water contact angle (WCA) analysis was realized in two steps, capturing the image via a digital camera followed by measuring the CA value through ImageJ software.

2.8 CysNO indirect measurements

For performing the reference measurements of CysNO, the colorimetric Griess method was adapted according to Peterson et al.[32] The Griess reagents were prepared by mixing 50 mmol L^{-1} sulfanilamide and 4 mmol L^{-1} NED (solubilized in citric acid) in a 1:1 (v/v) proportion. Then, aliquots of 1.5 mL (Griess solution) and 1.5 mL (target sample) were mixed. Analytical responses were performed using standard concentrations of nitrite ranging from 1 to 50 µmol L^{-1} and absorption detection at 510 nm. The serum sample was doped with CysNO at three concentrations (20, 40 and 80 µmol L-1) and recovery result was statistically compared to those values of CysNO measured by the proposed PES method.

3. Results and discussion

3.1 Fabrication of electrochemical paper-based sensor

In order to obtain the better interconnection between conductive ink and the insulating surface, different substrates have been explored, and materials such as cellulose-based (vegetal and chromatographic papers) and polystyrene films were carefully evaluated. The electrodes were manufactured via a stencil printed approach. Then, the morphological and electrochemical analysis were carefully performed. Morphological analysis by SEM involving cross-sectional views are exhibited in Figures 2A and S3 and the thickness values are estimated as 314, 226 and 206 µm for conductive ink deposited on vegetal paper, chromatographic material, and polystyrene film, respectively. While the polystyrene used as substrate exhibited poor adhesion with the conductive ink, the low thickness of carbon ink observed on chromatographic paper can be justified by the large porosities of these cellulose-based fibers (1 to 10 µm) in which the target ink disperses. On the other hand, the better thickness values of carbon ink measured on vegetal paper as insulating substrate can be due to a suitable interconnect between ABS and paraffin structures incorporated

under cellulose fibers, and the fact that waterproof paper does not have large porosities, as demonstrated in recent studies.[34,35]

So as to go deeper in this characterization, an electrochemical cleaning of the electrodes was performed on these three devices. Aiming at removing the residual and non-conductive material from the electrode surface, a cleaning process was performed upon the freshly manufactured electrode. This approach was adapted from recent study (cit) involving electrochemical oxidation in the presence of acetic acid solution (6.0 mol L^{-1}). Figure S4 presents the electrochemical response of the redox mediator $[Fe(CN)_6]^{3-/4-}$ that is extremely sensitive to chemical surface, on the non-cleaned and cleaned electrodes. The electrochemical parameters evaluated were peak-to-peak separation (ΔEp) and anodic peak current (i_{pa}).

Through CV measurements for electrodes constructed with chromatographic and polyester substrates , large ΔEp (170 to 180 mV) were observed probably due to the low conductivity of the electrode material.[36,37] However, the carbon-based ink decorated on vegetal paper revealed better redox parameters with a ΔEp of 101 mV and an increase of target current signal by 1.6 times, when compared with the electrodes manufactured on chromatographic and polyester substrates. Examples of binders that are gaining prominence in literature are mineral oil,[44] polystyrene,[45] glass varnish,[35,46] nail polish[47], starch (cit), native ABS(cit) and PDMS[48]. However, the carbon-based ink proposed herein makes possible the use of thermoplastic residues from 3D printed objects, showing the potential of this materials as low-cost binders, and most important the application of green chemistry's principles as preventing wastage and utilization of residues.

3.2 Electrochemical paper-based sensor characterization

As mentioned above the better results obtained in terms of ink thickness and electrochemical response were observed with the recycled conductive paste deposited on vegetal paper. In this way,

the electrical resistivity, as well as SEM, Raman and electrochemical analyses of the conductive surface were characterized in detail on this vegetal paper. The measured value of electrical resistivity of 68 ± 10 Ω cm is coherent with the traditional macroscopic information found in literature reported (≤ 1000 Ω cm).[37–41] This behavior can be associated to the intrinsic properties of graphite-based surfaces such as micrometer-size flakes, high-specific contact area, pore depth and greater electron accessibility, for example. It can also be linked to the elevated proportion of the conductive particles (ø ≤ 50 µm) on ABS binder (1:1; w/w) upon the vegetal paper.

Figure 2 presents SEM results in terms of thickness of the carbon-based composite (Figure 2A), interconnection between substrate and conductive ink (Figure 2B), and material surface before (Figure 2C) and after (Figure 2D) the electrochemical cleaning process. The images allow to estimate a thickness of 314 µm, the well-defined interconnection between the vegetal paper and the conductive material, and also the surface with partial removal of insulating ABS residues weakly adhering on the conductive trail.[22,42]

Figure 2E present the Raman measurements ranging from 1200 to 1800 cm^{-1} demonstrating distinct peak intensities at 1346 cm^{-1} and 1578 cm^{-1} as D and G bands, respectively.[43] These peaks can be attributed to sp^2 and sp^3 atoms hybridization in carbon-based composites and indicate that the calculated ratio of I_D/I_G = 0.142 is indeed in agreement with graphite-based inks prepared in well-known binder materials.[25]

Figures 2F and 2G summarize the cyclic voltammograms at different scan rates (10 to 100 mV s^{-1} associated with the redox behavior of $[Fe(CN)_6]^{3-/4-}$ exhibiting a value of ΔEp (96 ± 5 mV at 10 mV s^{-1}) that is characteristic of a quasi-reversible system.[49,50] A linear regression between scan rate and peak current (R^2 = 0.99) confirms that the electron mass-transfer is diffusional. Then, the calculated heterogeneous rate constant value was 2.0 (±0.1) x 10^{-3} cm s^{-1}, based on the Nicholson method (cit). Therefore, the proposed surface can be suitable as sensing material, similar to the other reported studies (cit).

The recycled electrodes were tested in different electrolytes of different pH values, i.e. 0.1 mol L^{-1} NaOH, KCl and H_2SO_4, as summarized in Figure S5. It is to be noted that the solid electrode does not show any faradaic activity (at potentials ranging from -0.5 V to 0.8 V vs C) involving contaminated species from conductive ink. The repeatability (number of cycles) and reproducibility (different PES microdevices) of the electrochemical response were then determined using $[Fe(CN)_6]^{3-/4-}$, as a model probe (see Figures 2H and 2I). The calculated statistical results of relative standard deviation (RSD) exhibit values of 4.6% (repeatability experiment; n=10) and 7.1% (reproducibility analysis; n=5). In addition, a one-way ANOVA (n=5) was performed on reproducibility responses, showing no significant difference between all manufactured devices (F-value = 1.33; p-value = 0.29; F-critical = 3.88), which suggests the potential for high-throughput manufacturing of these recycled carbon-based electrodes.

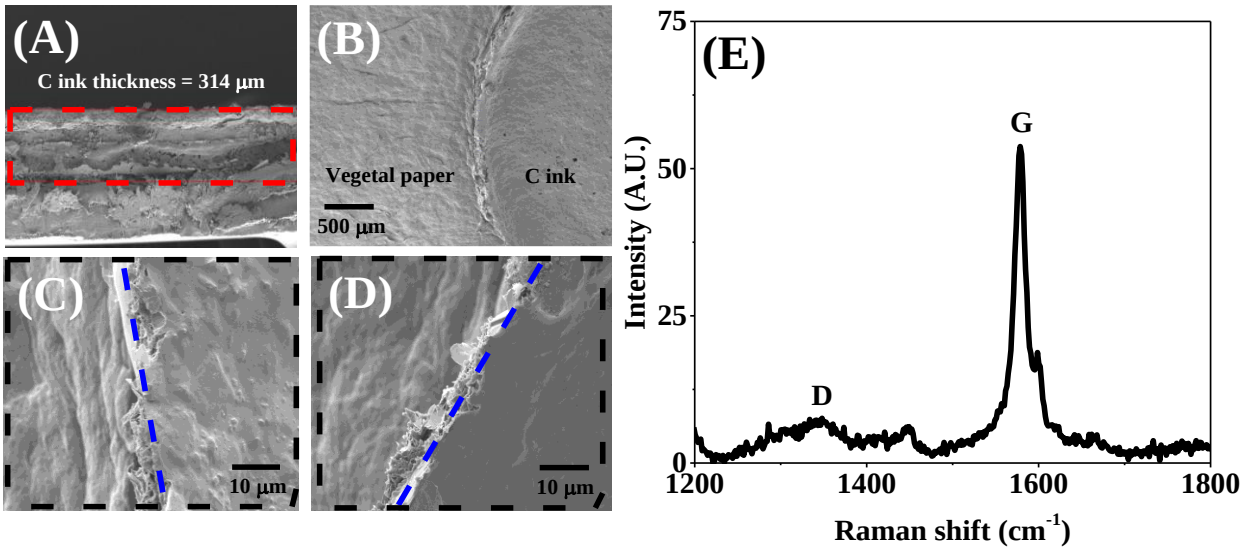

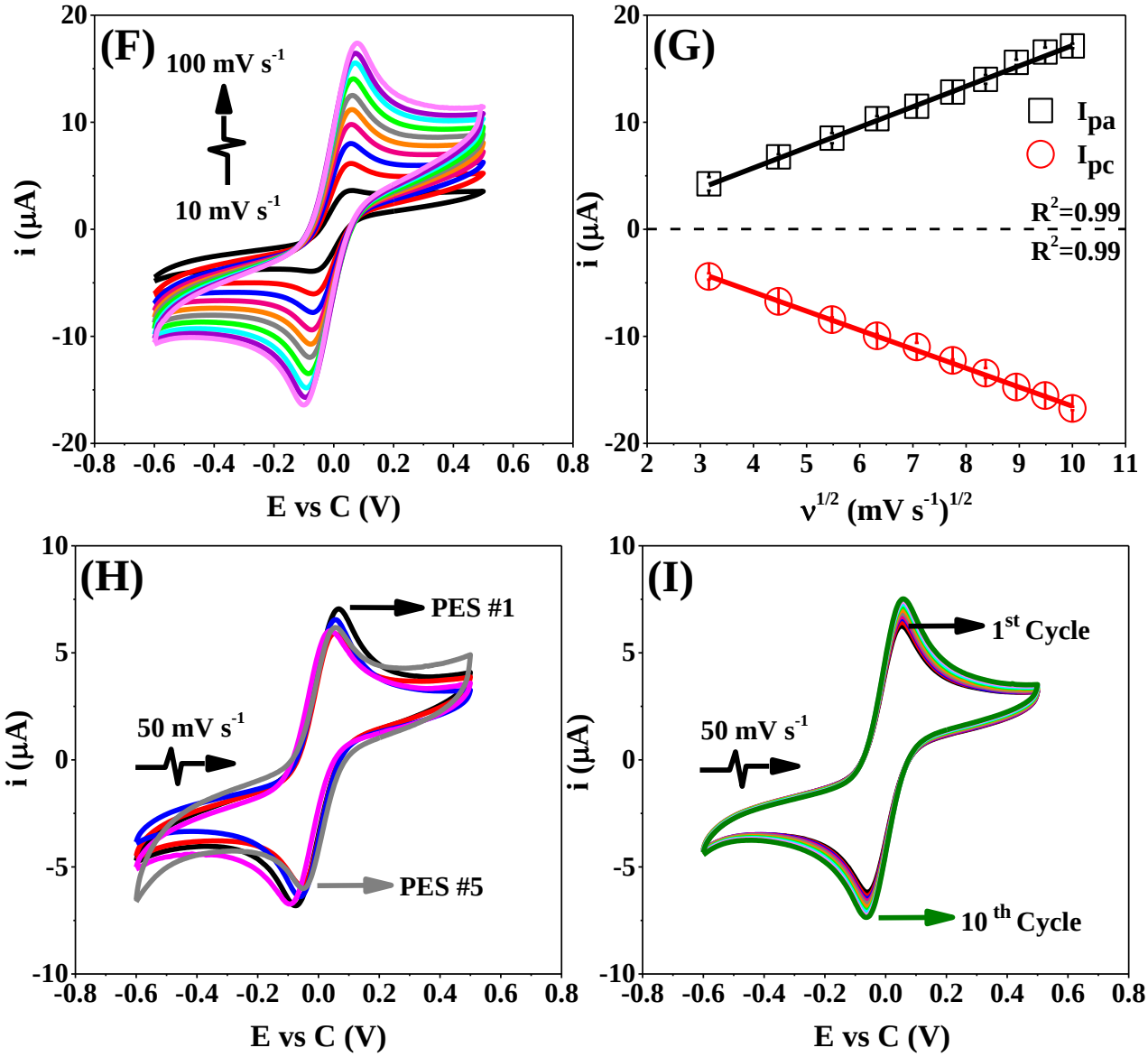

Figure 2. SEM measurements (A-D). Raman spectra (E). Cyclic voltammograms (F) and respective plots peak current intensity vs scan rate (G). Reproducibility (H) and repeatability (I) analysis.

3.3 Modification and characterization of the recycled electrodes for improving PES performances

Pure and applied studies involving solid state electrodes have demonstrated that the surface chemistry of allotrope carbon such as MWCNT and GO are important electrocatalyst materials (cit). Besides, the incorporation of nanostructured carbon with copper can improve the redox activities of nitrite, for example.[26] Therefore, the disposable recycled electrode surface was sequentially modified using a mixture of MWCNT/GO followed by electrochemical deposition of Cu. So as to

demonstrate the interest of such surface modification, it was characterized in terms of (i) interfacial tensions of the electrode surface via water contact angle (WCA) measurements and (ii) catalytic properties of the electrodes before and after the modification with Cu/MWCNT/GO via CV electrochemical experiments on nitrite solutions. As a matter of comparison, similar studies were conducted using 3D printed carbon black sensor, including WCA (Figure S6) and catalytic responses (Figure 3).

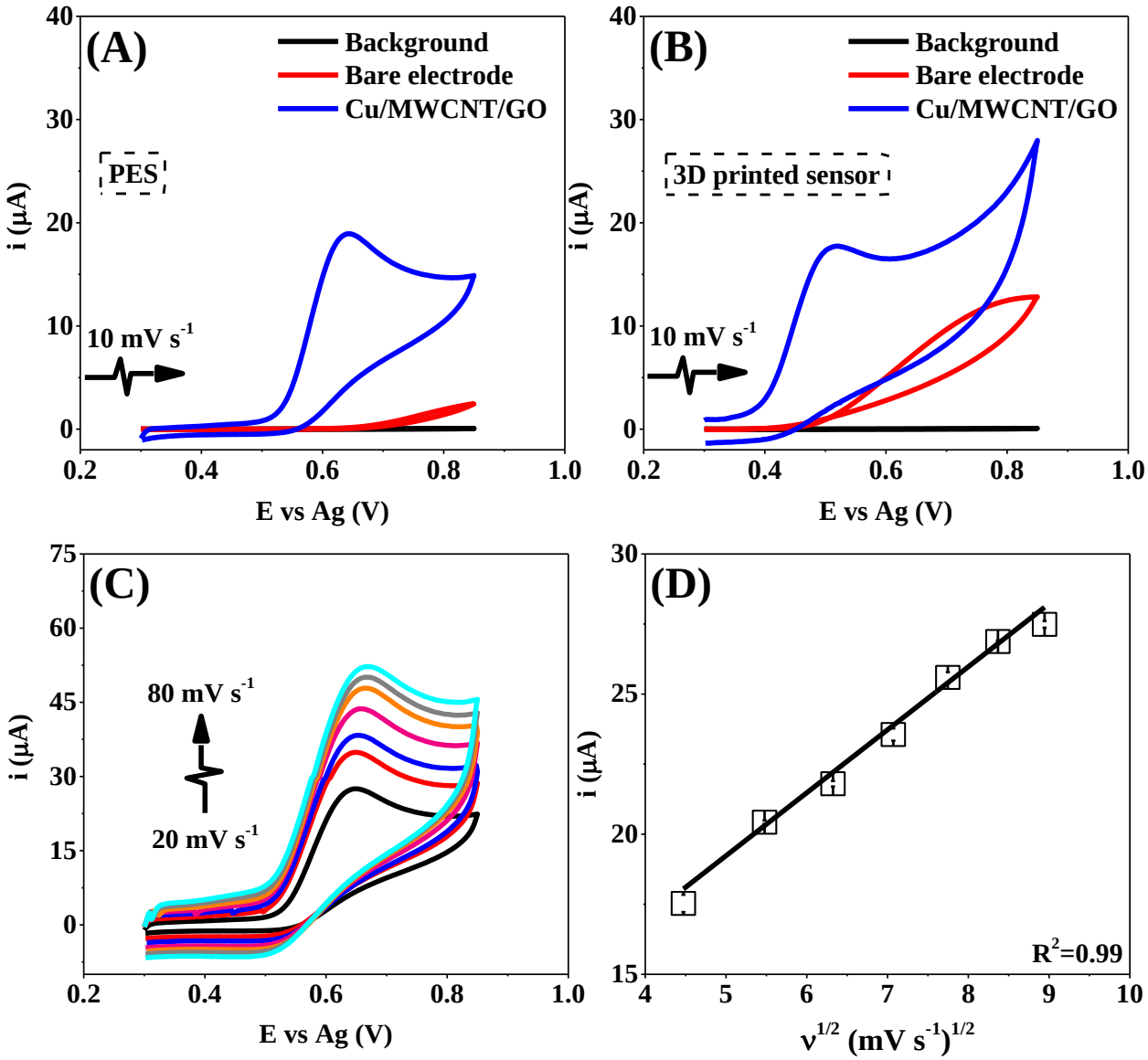

Figure 3. Electrochemical behavior of nitrite before and after the surface modification involving PES (A) and 3D printed sensor (B). Influence of different scan rates in the faradaic peak signal of nitrite oxidation (C-D) on the PES sensor. Error bars are associated with standard deviation from three experiments.

WCA measurement on bare PES and 3D-printed surface showed values of 88 ± 3 and 85 ± 3º, respectively, indicating that both heterogeneous interfaces exhibited equivalent hydrophilic character. When both electrodes are modified with Cu/MWCNT/GO structure, the WCA values shift to 60 ± 3 and 56 ± 3º . These values are still statistically indifferent (paired t-test; p = 0.05) as expected as the modification process and nature is the same. Furthermore, these WCA values lower than 90° indicate a compatibility of these electrodes for performing drop-cast experiment and stationary measurements, for example.

As observed in Figures 3A-B, the evaluated electrochemical behavior indicated that both devices showed well-defined peak and acceptable catalytic behavior for nitrite oxidation at 0.63 and 0.51 V vs Ag, respectively. In addition, the electrochemical signals of the modified exlectrodes are enhanced by 6.3 and 4.8 times for the proposed device and 3D-printed electrode, respectively. These comparative experiments successfully demonstrate that both kinetic regimes are irreversible.[26,49,50]

Thus, the electrode surface covered with Cu/MWCNT/GO nanostructures shows excellent catalytic properties for the oxidation of nitrite when compared with responses obtained upon bare electrodes. Bagheri et al.[26] reported glass carbon electrode decorated with Cu/reduced GO/MWCNT for drastic improvement of the nitrite and nitrate oxidations. The authors showed that the best redox activities exhibited by Cu/reduced GO/MWCNT surface can be explained by the large surface area, action sites, and a high number of edges and defects.

As it can be seen in Figures 3C-D and S7, other comparative studies were performed using both modified electrodes with cyclic voltammograms of what? at scan rates ranging from 20 to 80 mV s^{-1}. The obtained plots in terms of peak current vs scan rate successfully indicate that the redox process is diffusion-controlled.[51]

We also investigated the performance of the modified surface in terms of reproducibility and repeatability of the electrochemical signal using the oxidation of nitrite, as model reaction. These studies were realized via three different devices and through five measurements in sequence (Figure

4). The recorded electrochemical data when provide respective RSD values of 3.4 and 1.8% for repeatability and reproducibility analysis, demonstrating the suitable performance of the PES decorated with Cu/MWCNT/GO.

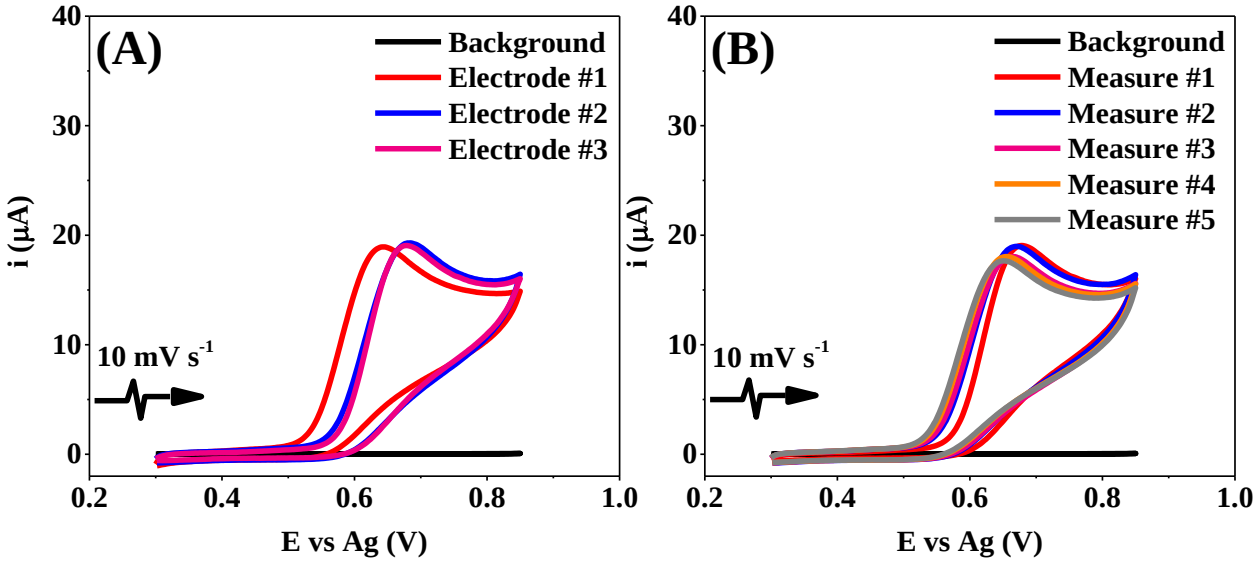

Figure 4. Catalytic performance of modified electrodes to oxidation of nitrite in term of reproducibility (A) and repeatability (B) measurements.

3.4 Recycled PES for sensing CySNO

As the electrode proposed herein exhibits satisfactory performance for the oxidation of nitrite, we explored those redox properties to achieve the indirect analysis of low molecular weight RSNOs. RSNO can be converted to nitrite through many strategies of decomposition, making possible the use of nitrite as indirect marker.[28] For this reason, chronoamperometry was selected for evaluating the possibility of indirect detection of CySNO in three different steps: (i) the use of standard nitrite to calibrate the electrode, (ii) the use of pre decomposed CySNO in supporting

electrolyte and (iii) the use of pre decomposed CySNO prepared in diluted serum samples and in supporting electrolyte (which rate? Wifh supporting electrolyte . All analytical responses were performed at a detection potential 0.6 V vs Ag for 50 s with nitrite concentrations ranging from 10 to 125 µmol L^{-1}. The obtained chronoamperograms and respective plots (current signal vs concentration) are presented in Figures 5A-D. It is important to mention that we also realized parallel amperometric experiments through fully 3D printed electrodes with detection potential at 0.5 V for 30 s (see the analytical curve in Figure S8 in the SI).

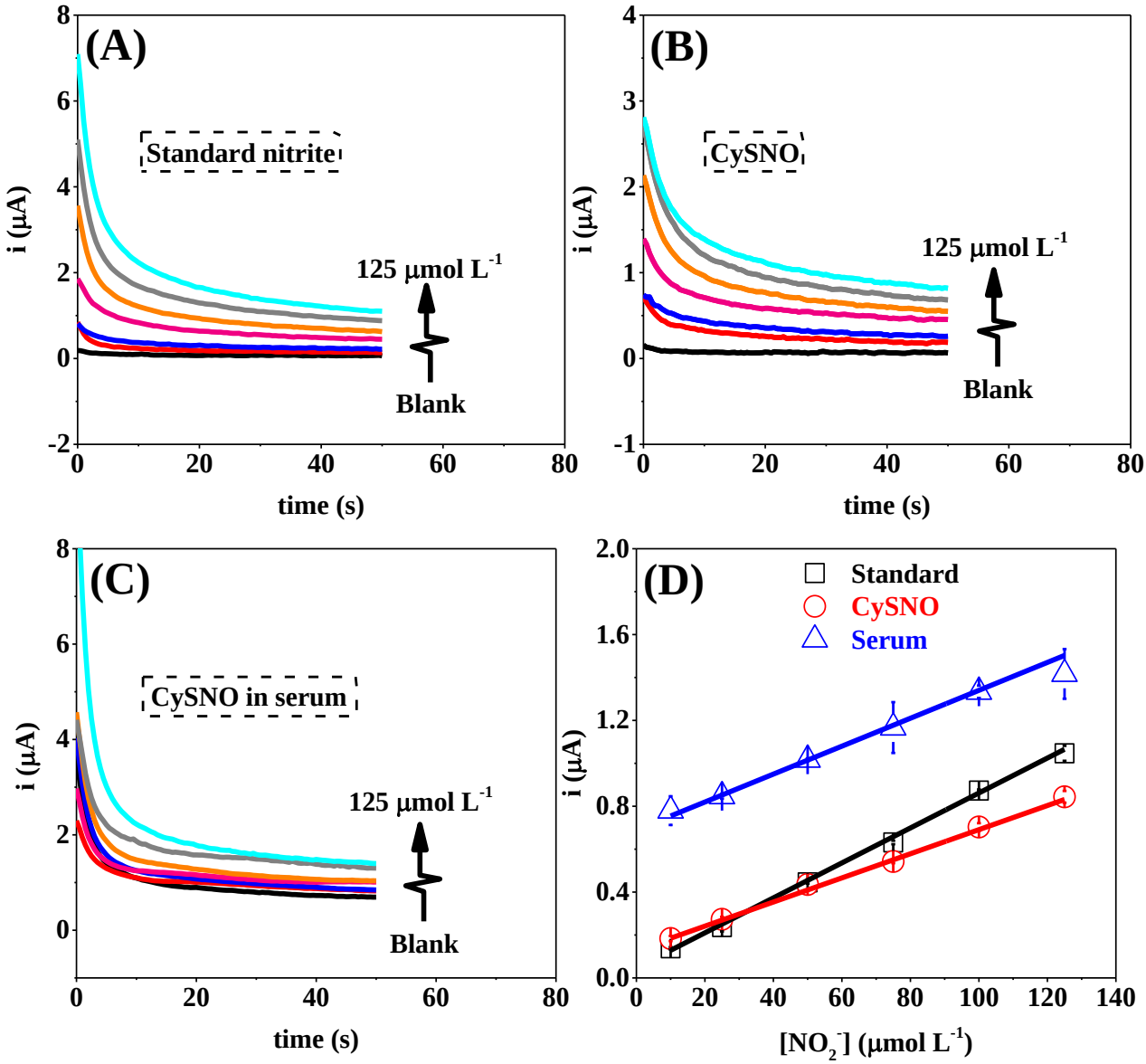

Figure 5. Chronoamperogram of standard nitrite solutions (A), decomposed CySNO (B), decomposed CySNO, prepared in diluted serum samples (C) and respective analytical responses ranging from 10 to 125 µmol L^{-1} (D). Error bars it is associate to standard deviation from three experiments.

Under amperometric conditions, the linear regression associated to detection of nitrite and CySNO exhibited a good R^2 value (0.99) and similar analytical sensitivity with values 0.008 and 0.005 µA/[µmol L^{-1}], indicating that the present electroanalytical method can be performed to indirect analysis of CySNO. As can be seen in Figure S7, the electrochemical performance with modified 3D-printed sensor showed values of R^2 = 0.99 and sensitivity of 0.002 µA/[µmol L^{-1}] in the same order as those obtained for Cu/MWCNT/GO modified PES. Furthermore, quantitative analysis for the sample composed of decomposed CySNO in diluted serum samples (Figure 5C and D) indicated sensitivity level of 0.006 µA/[µmol L^{-1}] that is similar to sensing properties observed on amperometric measurements in the absence of complex biological matrix.

The estimated limit of detection (LOD) values to indirect detection of CySNO in standard and serum samples were 4.4 and 4.1 µmol L^{-1}, respectively. (LOD was calculated using the 3.3*SD_{blank}/slope of analytical curve). Duarte-Junior et al.[52] proposed a microfluidic device with integrated electrochemical detector for separating and detecting RSNOs, after a decomposition to nitrite based on mercury with LODs of 20 µmol L^{-1}. Ismail et al.[33] further constructed a microfluidic paper-based microdevice for indirect colorimetric detection of RSNOs, with the same decomposition protocol with a LOD of 4 µmol L^{-1}.

In another study, Rebecca et al.[53] manufactured a microfluidic device combined with platinum electrode for amperometric analysis of RSNOs. For facilitating the photolysis of nitrosothiol groups and realizing the amperometric detection of nitrite, the authors reported a simple degradation through UV-LED and an analysis with a procedure time low than 2 min and LOD value of 73 nmol L^{-1}. Here, the proposed modified PES provides suitable detectability for CySNO and the estimated LOD is better or similar when compared to low-cost analytical tools (you must put

referecnes then). Also, the herein reported linear concentration range (10-125 µmol L^{-1}) can be useful to clinical application that involved Parkinson's disease. (cit)

3.5 Selectivity of the recycled PES

Nitrite analysis in biological matrix can be susceptible to any interference, as biomolecules and ions are commonly found in biological fluids associated to sensing applications in terms of RSNOs-based analysis.[27,28,30] The selectivity of Cu/MWCNT/GO/PES as nitrite sensor was investigated by amperommetric measurements of nitrite in the absence and presence of nitrate, uric acid, chloride and Fe(II) with a proportion of 1:10. The electrochemical responses before and after the addition of interfering compounds are presented in Figures 6A-B, with interference levels of -11, -2, -0.6 and 3% for nitrate, uric acid, chloride and Fe(II), respectively. We observed that the redox activity of nitrite is not drastically influenced by the presence of the above mentioned interference compounds, denoting the great potential of the modified electrodes to analysis of CysNO in complex biological compound.

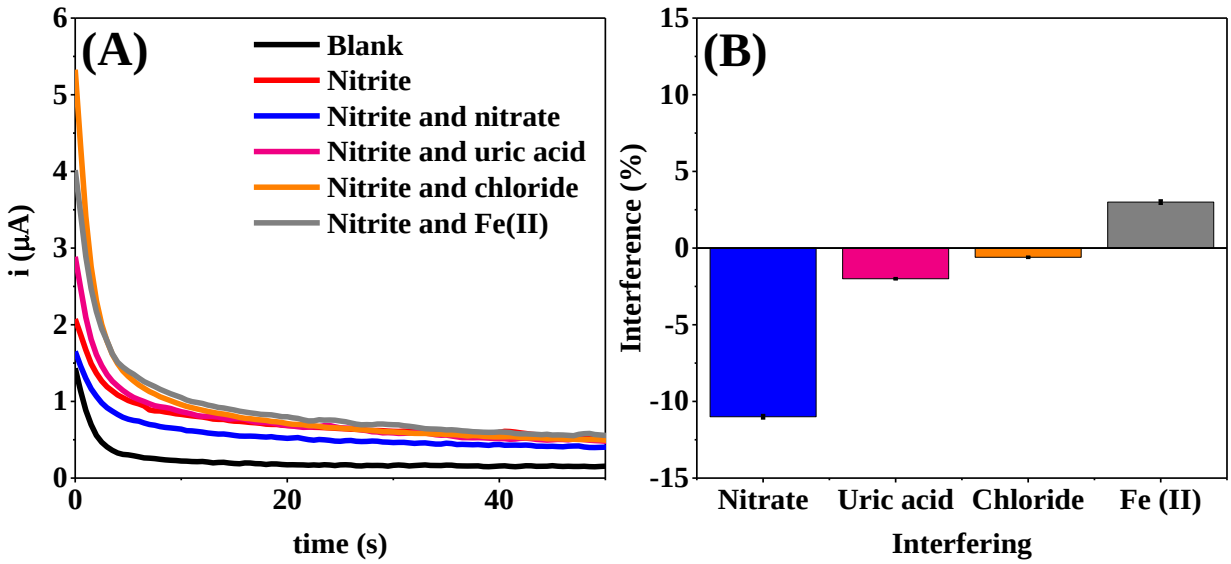

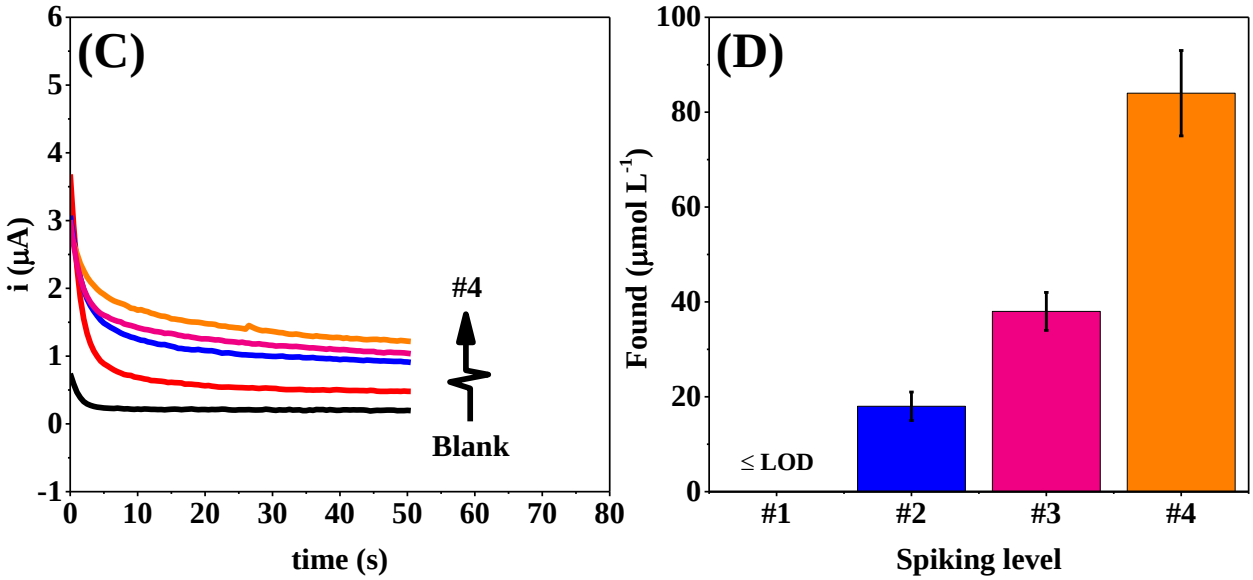

Figure 6. Electrochemical responses (A) and respective histogram (B) of the selectivity of PES. Cronoamperograms results in the absence and presence of decomposed CySNO samples #1 (diluted serum), #2 (serum dopped with 20 μmol L^{-1}), #3 (serum dopped with 40 μmol L^{-1}) and #4 (serum dopped with 80 μmol L^{-1}) (C). Respective histograms involving the measured value of CySNO in serum samples (D). Error bars are associated to standard deviation from three experiments.

3.6 Sample analysis

To demonstrate the feasibility of the manufactured electrochemical device as CysNO sensor in human serum samples, the Cu/MWCNT/GO/PES was tested in terms of recovery measurements through the addition of three different levels of decomposed CysNO into artificial serum samples, 20, 40 and 80 μmol L^{-1}, as indicated in Figures 6C-D. All obtained amperometric responses exhibited recovery values ranging from 90 to 105% (see summarized results in Table 1). The same experiments were performed using the Griess-colorimetric method,[32] with similar samples preparation step. Summarized responses under both instrumental systems showed detected levels of CysNO without statistical difference (paired t-test; p=0.05), indicating that the proposed recycled PES allows quantitation with equivalent performance as for reference method.

Table 1. Recovery experiment involving serum samples doped CysNO in different concentrations with the PES microdevice and the Griess-method.

Experiments	Added ($\mu mol\ L^{-1}$)	Found ($\mu mol\ L^{-1}$)		Recovery (%)
		PES	Griess-method	
#1	-	≤ LOD	≤ LOD	-
#2	20	18 ± 3	19.1 ± 0.5	90
#3	40	38 ± 4	37.4 ± 0.5	95
#4	80	84 ± 9	76.4 ± 0.5	105

4. Conclusions

We demonstrated for the first time the performance of recycled electrodes for paper-based sensors, composed of ABS residues and graphite flakes, making it a potential valuable protocol for recycling thermoplastic waste from 3D-printing industry, according to the green chemical principles. We demonstrated the huge performance of the recycled composite as binder structure through: (i) Detailed macroscopic, microscopic, and electrochemical characterizations confirm that the recycled ABS is a great alternative for constructing conductive ink; (ii) The comparative study between the proposed sensor and a fully 3D-printed device has shown similar faradaic performance, indicating that the recycled and disposable electrode proposed herein can be explored to electrocatalysis; (iii) The proposed electrochemical cell when combined with electrochemical detector has successfully demonstrated huge potential to indirect analysis of S-nitrosothiol in diluted serum samples. Therefore, this cleaner approach for reusing complex thermoplastic materials to future fabrication of conductive ink is attractive in order to overcome the vast number of ABS residues. In addition, the proposed recyclable method for manufacturing paper-based sensor allows low-cost materials and green chemical principles, opening novel opportunities in the modern chemical sensor field dedicates to biological applications.

Acknowledgments

The authors would like to thank CAPES, CNPq (grants 426496/2018-3, 308140/2016-8, 307554/2020-1 and 142412/2020-1) and INCTBio (grant 465389/2014-7) for the financial support and granted scholarships. The authors acknowledge the Multi-user Laboratory of high-resolution microscopy (LabMic/UFG), PhD. Lucas C. Duarte and Professor Paulo Sergio for using their facilities during (SEM and Raman) measurements, technical supporting for solubilize the ABS residue and technical apport during the spectrophotometric analysis, respectively.

References

(1) Furet, B.; Poullain, P.; Garnier, S. 3D Printing for Construction Based on a Complex Wall of Polymer-Foam and Concrete. *Addit. Manuf.* **2019**, *28* (September 2018), 58–64. https://doi.org/10.1016/j.addma.2019.04.002.

(2) Mirdamadi, E.; Tashman, J. W.; Shiwarski, D. J.; Palchesko, R. N.; Feinberg, A. W. FRESH 3D Bioprinting a Full-Size Model of the Human Heart. *ACS Biomater. Sci. Eng.* **2020**, 0–6. https://doi.org/10.1021/acsbiomaterials.0c01133.

(3) Ngo, T. D.; Kashani, A.; Imbalzano, G.; Nguyen, K. T. Q.; Hui, D. Additive Manufacturing (3D Printing): A Review of Materials, Methods, Applications and Challenges. *Compos. Part B Eng.* **2018**, *143* (February), 172–196. https://doi.org/10.1016/j.compositesb.2018.02.012.

(4) Ambrosi, A.; Webster, R. D.; Pumera, M. Electrochemically Driven Multi-Material 3D-Printing. *Appl. Mater. Today* **2020**, *18*, 100530. https://doi.org/10.1016/j.apmt.2019.100530.

(5) Global 3D Printing Filament Market is Anticipated to Grow at a CAGR of 31.10% during the Forecast Period from 2021 to 2030, GlobeNewswire (2021). https://www.globenewswire.com/news-release/2021/12/27/2358043/0/en/Global-3D-Printing-

Filament-Market-is-Anticipated-to-Grow-at-a-CAGR-of-31-10-during-the-Forecast-Period-from-2021-to-2030-Quince-Market-Insights.html.

(6) O'Neil, G. D. Toward Single-Step Production of Functional Electrochemical Devices Using 3D Printing: Progress, Challenges, and Opportunities. *Curr. Opin. Electrochem.* **2020**, *20*, 60–65. https://doi.org/10.1016/j.coelec.2020.02.023.

(7) Kalsoom, U.; Nesterenko, P. N.; Paull, B. Current and Future Impact of 3D Printing on the Separation Sciences. *TrAC - Trends Anal. Chem.* **2018**, *105*, 492–502. https://doi.org/10.1016/j.trac.2018.06.006.

(8) Ambrosi, A.; Pumera, M. 3D-Printing Technologies for Electrochemical Applications. *Chem. Soc. Rev.* **2016**, *45* (10), 2740–2755. https://doi.org/10.1039/c5cs00714c.

(9) Cardoso, R. M.; Kalinke, C.; Rocha, R. G.; dos Santos, P. L.; Rocha, D. P.; Oliveira, P. R.; Janegitz, B. C.; Bonacin, J. A.; Richter, E. M.; Munoz, R. A. A. Additive-Manufactured (3D-Printed) Electrochemical Sensors: A Critical Review. *Anal. Chim. Acta* **2020**, *1118*, 73–91. https://doi.org/10.1016/j.aca.2020.03.028.

(10) Mohamad Nasir, M. Z.; Pumera, M. Emerging Mono-Elemental 2D Nanomaterials for Electrochemical Sensing Applications: From Borophene to Bismuthene. *TrAC - Trends Anal. Chem.* **2019**, *121*. https://doi.org/10.1016/j.trac.2019.115696.

(11) Hamzah, H. H.; Shafiee, S. A.; Abdalla, A.; Patel, B. A. 3D Printable Conductive Materials for the Fabrication of Electrochemical Sensors: A Mini Review. *Electrochem. commun.* **2018**, *96* (August), 27–31. https://doi.org/10.1016/j.elecom.2018.09.006.

(12) Katseli, V.; Economou, A.; Kokkinos, C. A Novel All-3D-Printed Cell-on-a-Chip Device as a Useful Electroanalytical Tool: Application to the Simultaneous Voltammetric Determination of Caffeine and Paracetamol. *Talanta* **2020**, *208* (July 2019), 120388.

https://doi.org/10.1016/j.talanta.2019.120388.

(13) Mikula, K.; Skrzypczak, D.; Izydorczyk, G.; Warchoł, J.; Moustakas, K.; Chojnacka, K.; Witek-Krowiak, A. 3D Printing Filament as a Second Life of Waste Plastics—a Review. *Environ. Sci. Pollut. Res.* **2021**, *28* (10), 12321–12333. https://doi.org/10.1007/s11356-020-10657-8.

(14) Gkartzou, E.; Koumoulos, E. P.; Charitidis, C. A. Production and 3D Printing Processing of Bio-Based Thermoplastic Filament. *Manuf. Rev.* **2017**, *4*. https://doi.org/10.1051/mfreview/2016020.

(15) Ligon, S. C.; Liska, R.; Gurr, M.; Mu, R.; Gmbh, H. B. F. D.; Bleiche, A. D. R.; D-, L. Polymers for 3D Printing and Customized Additive Manufacturing. *Chem. Rev.* **2017**, No. 117, 10212–10290. https://doi.org/10.1021/acs.chemrev.7b00074.

(16) Anastas, P.; Eghbali, N. Green Chemistry : Principles and Practice. *Chem. Soc. Rev.* **2010**, 301–312. https://doi.org/10.1039/b918763b.

(17) Tian, X.; Liu, T.; Wang, Q.; Dilmurat, A.; Li, D.; Ziegmann, G. Recycling and Remanufacturing of 3D Printed Continuous Carbon Fiber Reinforced PLA Composites. *J. Clean. Prod.* **2017**, *142*, 1609–1618. https://doi.org/10.1016/j.jclepro.2016.11.139.

(18) Rahimizadeh, A.; Kalman, J.; Fayazbakhsh, K.; Lessard, L. Recycling of Fiberglass Wind Turbine Blades into Reinforced Filaments for Use in Additive Manufacturing. *Compos. Part B Eng.* **2019**, *175* (July), 107101. https://doi.org/10.1016/j.compositesb.2019.107101.

(19) Khorablou, Z.; Shahdost-fard, F.; Razmi, H.; Yola, M. L.; Karimi-Maleh, H. Recent Advances in Developing Optical and Electrochemical Sensors for Analysis of Methamphetamine: A Review. *Chemosphere* **2021**, *278*. https://doi.org/10.1016/j.chemosphere.2021.130393.

(20) de Araujo, W. R.; Cardoso, T. M. G.; da Rocha, R. G.; Santana, M. H. P.; Muñoz, R. A. A.;

Richter, E. M.; Paixão, T. R. L. C.; Coltro, W. K. T. Portable Analytical Platforms for Forensic Chemistry: A Review. *Anal. Chim. Acta* **2018**, *1034*, 1–21. https://doi.org/10.1016/j.aca.2018.06.014.

(21) Cate, D. M.; Noblitt, S. D.; Volckens, J.; Henry, C. S. Multiplexed Paper Analytical Device for Quantification of Metals Using Distance-Based Detection. *Lab Chip* **2015**, *15* (13), 2808–2818. https://doi.org/10.1039/c5lc00364d.

(22) Silva-Neto, H. A.; Santhiago, M.; Duarte, L. C.; Coltro, W. K. T. Fully 3D Printing of Carbon Black-Thermoplastic Hybrid Materials and Fast Activation for Development of Highly Stable Electrochemical Sensors. *Sensors Actuators B Chem.* **2021**, *349* (May), 130721. https://doi.org/10.1016/j.snb.2021.130721.

(23) Bao, C.; Kaur, M.; Kim, W. S. Toward a Highly Selective Artificial Saliva Sensor Using Printed Hybrid Field Effect Transistors. *Sensors Actuators, B Chem.* **2019**, *285* (January), 186–192. https://doi.org/10.1016/j.snb.2019.01.062.

(24) Song, Y.; Xu, T.; Xiu, J.; Zhang, X. Mini-Pillar Microarray for Individually Electrochemical Sensing in Microdroplets. *Biosens. Bioelectron.* **2020**, *149*. https://doi.org/10.1016/j.bios.2019.111845.

(25) Noviana, E.; McCord, C. P.; Clark, K. M.; Jang, I.; Henry, C. S. Electrochemical Paper-Based Devices: Sensing Approaches and Progress toward Practical Applications. *Lab Chip* **2020**, *20* (1), 9–34. https://doi.org/10.1039/c9lc00903e.

(26) Bagheri, H.; Hajian, A.; Rezaei, M.; Shirzadmehr, A. Composite of Cu Metal Nanoparticles-Multiwall Carbon Nanotubes-Reduced Graphene Oxide as a Novel and High Performance Platform of the Electrochemical Sensor for Simultaneous Determination of Nitrite and Nitrate. *J. Hazard. Mater.* **2017**, *324*, 762–772. https://doi.org/10.1016/j.jhazmat.2016.11.055.

(27) Williams, D. L. Y. N. H. The Chemistry of S-Nitrosothiols. *Anal. Chem.* **1999**, *32* (10), 869–876.

(28) Bedioui, F.; Ismail, A.; Griveau, S. Electrochemical Detection of Nitric Oxide and S-Nitrosothiols in Biological Systems : Past , Present & Future. *Curr. Opin. Electrochem.* **2018**, *12*, 42–50. https://doi.org/10.1016/j.coelec.2018.04.014.

(29) Cardenas, A. J. P.; Abelman, R.; Warren, T. H. Conversion of Nitrite to Nitric Oxide at Zinc via S-Nitrosothiols†. *Chem. Commun.* **2014**, *2* (6), 168–170. https://doi.org/10.1039/c3cc46102e.

(30) Oliveira, M. G. De; Shishido, M.; Seabra, A. B.; Morgon, N. H. Thermal Stability of Primary S -Nitrosothiols : Roles of Autocatalysis and Structural Effects on the Rate of Nitric Oxide Release. *J. Phys. Chem. A* **2002**, 8963–8970.

(31) Veleeparampil, M. M.; Aravind, U. K.; Aravindakumar, C. T. Decomposition of S-Nitrosothiols Induced by UV and Sunlight. *Adv. Phys. Chem.* **2009**. https://doi.org/10.1155/2009/890346.

(32) Peterson, L. A.; Wagener, T.; Sies, H.; Stahl, W. Decomposition of S -Nitrosocysteine via S - to N -Transnitrosation. *Chem. Res. Toxicol.* **2007**, 721–723.

(33) Ismail, A.; Araújo, M. O.; Chagas, C. L. S.; Griveau, S.; D'Orlyé, F.; Varenne, A.; Bedioui, F.; Coltro, W. K. T. Colorimetric Analysis of the Decomposition of S-Nitrosothiols on Paper-Based Microfluidic Devices. *Analyst* **2016**, *141* (22), 6314–6320. https://doi.org/10.1039/c6an01439a.

(34) Camargo, J. R.; Andreotti, I. A. A.; Kalinke, C.; Henrique, J. M.; Bonacin, J. A.; Janegitz, B. C. Talanta Waterproof Paper as a New Substrate to Construct a Disposable Sensor for the Electrochemical Determination of Paracetamol and Melatonin. *Talanta* **2020**, *208* (October 2019), 120458. https://doi.org/10.1016/j.talanta.2019.120458.

(35) Habdias A. Silva-Neto; Cardoso, T. M. G.; McMahon, C. J.; Sgobbi, L. F.; Henry, C. S.; Coltro, W. K. T. Plug-and-Play Assembly of Paper-Based Colorimetric and Electrochemical Devices for Multiplexed Detection of Metals†. *Analyst* **2021**, *146* (11). https://doi.org/10.1039/d1an00176k.

(36) Santhiago, M.; Corrêa, C. C.; Bernardes, J. S.; Pereira, M. P.; Oliveira, L. J. M.; Strauss, M.; Bufon, C. C. B. Flexible and Foldable Fully-Printed Carbon Black Conductive Nanostructures on Paper for High-Performance Electronic, Electrochemical, and Wearable Devices. *ACS Appl. Mater. Interfaces* **2017**, *9* (28), 24365–24372. https://doi.org/10.1021/acsami.7b06598.

(37) Silva, L. A. J.; da Silva, W. P.; Giuliani, J. G.; Canobre, S. C.; Garcia, C. D.; Munoz, R. A. A.; Richter, E. M. Use of Pyrolyzed Paper as Disposable Substrates for Voltammetric Determination of Trace Metals. *Talanta* **2017**, *165* (October 2016), 33–38. https://doi.org/10.1016/j.talanta.2016.12.009.

(38) Noviana, E.; McCord, C.; Clark, K.; Jang, I.; Henry, C. Electrochemical Paper-Based Devices: Sensing Approaches and Progress Toward Practical Applications. *Lab Chip* **2019**. https://doi.org/10.1039/C9LC00903E.

(39) Rocha, D. S.; Duarte, L. C.; Silva-Neto, H. A.; Chagas, C. L. S.; Santana, P.; Filho, N. R. A.; Coltro, W. K. T. Sandpaper-Based Electrochemical Devices Assembled on a Reusable 3D-Printed Holder to Detect Date Rape Drug in Beverages. *Talanta* **2021**, *232* (April). https://doi.org/10.1016/j.talanta.2021.122408.

(40) Stefano, J. S.; Orzari, L. O.; Silva-neto, H. A.; Ataíde, V. N. De; Mendes, L. F.; Karlos, W.; Coltro, T.; Regis, T.; Cesar, L.; Janegitz, B. C. Different Approaches for Fabrication of Low-Cost Electrochemical Sensors. *Curr. Opin. Electrochem.* **2022**, *32*, 100893. https://doi.org/10.1016/j.coelec.2021.100893.

(41) Petroni, J. M.; Neves, M. M.; de Moraes, N. C.; Bezerra da Silva, R. A.; Ferreira, V. S.;

Lucca, B. G. Development of Highly Sensitive Electrochemical Sensor Using New Graphite/Acrylonitrile Butadiene Styrene Conductive Composite and 3D Printing-Based Alternative Fabrication Protocol. *Anal. Chim. Acta* **2021**, *1167*. https://doi.org/10.1016/j.aca.2021.338566.

(42) Richter, E. M.; Rocha, D. P.; Cardoso, R. M.; Keefe, E. M.; Foster, C. W.; Munoz, R. A. A.; Banks, C. E. Complete Additively Manufactured (3D-Printed) Electrochemical Sensing Platform. *Anal. Chem.* **2019**, *91*, 12844–12851. https://doi.org/10.1021/acs.analchem.9b02573.

(43) Caṇado, L. G.; Takai, K.; Enoki, T.; Endo, M.; Kim, Y. A.; Mizusaki, H.; Jorio, A.; Coelho, L. N.; Magalhães-Paniago, R.; Pimenta, M. A. General Equation for the Determination of the Crystallite Size La of Nanographite by Raman Spectroscopy. *Appl. Phys. Lett.* **2006**, *88* (16), 1–4. https://doi.org/10.1063/1.2196057.

(44) Mettakoonpitak, J.; Mehaffy, J.; Volckens, J.; Henry, C. S. AgNP/Bi/Nafion-Modified Disposable Electrodes for Sensitive Zn(II), Cd(II), and Pb(II) Detection in Aerosol Samples. *Electroanalysis* **2017**, *29* (3), 880–889. https://doi.org/10.1002/elan.201600591.

(45) Rymansaib, Z.; Iravani, P.; Emslie, E.; Medvidović-Kosanović, M.; Sak-Bosnar, M.; Verdejo, R.; Marken, F. All-Polystyrene 3D-Printed Electrochemical Device with Embedded Carbon Nanofiber-Graphite-Polystyrene Composite Conductor. *Electroanalysis* **2016**, *28* (7), 1517–1523. https://doi.org/10.1002/elan.201600017.

(46) Pradela-Filho, L. A.; Andreotti, I. A. A.; Carvalho, J. H. S.; Araújo, D. A. G.; Orzari, L. O.; Gatti, A.; Takeuchi, R. M.; Santos, A. L.; Janegitz, B. C. Glass Varnish-Based Carbon Conductive Ink: A New Way to Produce Disposable Electrochemical Sensors. *Sensors Actuators B Chem.* **2020**, *305*, 127433. https://doi.org/10.1016/j.snb.2019.127433.

(47) Pradela-filho, L. A.; Araújo, D. A. G.; Takeuchi, R. M.; Santos, A. L. Nail Polish and Carbon Powder : An Attractive Mixture to Prepare Paper-Based Electrodes. *Electrochim. Acta* **2017**,

258, 786–792. https://doi.org/10.1016/j.electacta.2017.11.127.

(48) Sameenoi, Y.; Mensack, M. M.; Boonsong, K.; Ewing, R.; Dungchai, W.; Chailapakul, O.; Cropek, D. M.; Henry, C. S. Poly(Dimethylsiloxane) Cross-Linked Carbon Paste Electrodes for Microfluidic Electrochemical Sensing. *Analyst* **2011**, *136* (15), 3177–3184. https://doi.org/10.1039/c1an15335h.

(49) McCreery, R. L. Advanced Carbon Electrode Materials for Molecular Electrochemistry. *Chem. Rev.* **2008**, *108* (7), 2646–2687. https://doi.org/10.1021/cr068076m.

(50) Nicholson, R. S.; Shain, I. Theory of Stationary Electrode Polarography Single Scan and Cyclic Methods Applied to Reversible , Irreversible , and Kinetic Systems. *Anal. Chem.* **1964**, *36* (4), 706–723. https://doi.org/10.1021/ac60210a007.

(51) Santos, W. J. R.; Sousa, A. L.; Luz, R. C. S.; Damos, F. S.; Kubota, L. T.; Tanaka, A. A.; Tanaka, S. M. C. N. Amperometric Sensor for Nitrite Using a Glassy Carbon Electrode Modified with Alternating Layers of Iron(III) Tetra-(N-Methyl-4-Pyridyl)-Porphyrin and Cobalt(II) Tetrasulfonated Phthalocyanine. *Talanta* **2006**, *70* (3), 588–594. https://doi.org/10.1016/j.talanta.2006.01.023.

(52) Duarte-Junior, G. F.; Ismail, A.; Griveau, S.; D'Orlyé, F.; Fracassi Da Silva, J. A.; Coltro, W. K. T.; Bedioui, F.; Varenne, A. Integrated Microfluidic Device for the Separation, Decomposition and Detection of Low Molecular Weight S-Nitrosothiols. *Analyst* **2019**, *144* (1), 180–185. https://doi.org/10.1039/c8an00757h.

(53) Hunter, R. A.; Schoen, M. H. S - Nitrosothiol Analysis via Photolysis and Amperometric Nitric Oxide Detection in a Micro Fl Uidic Device. *Anal. Chem.* **2015**. https://doi.org/10.1021/ac503220z.